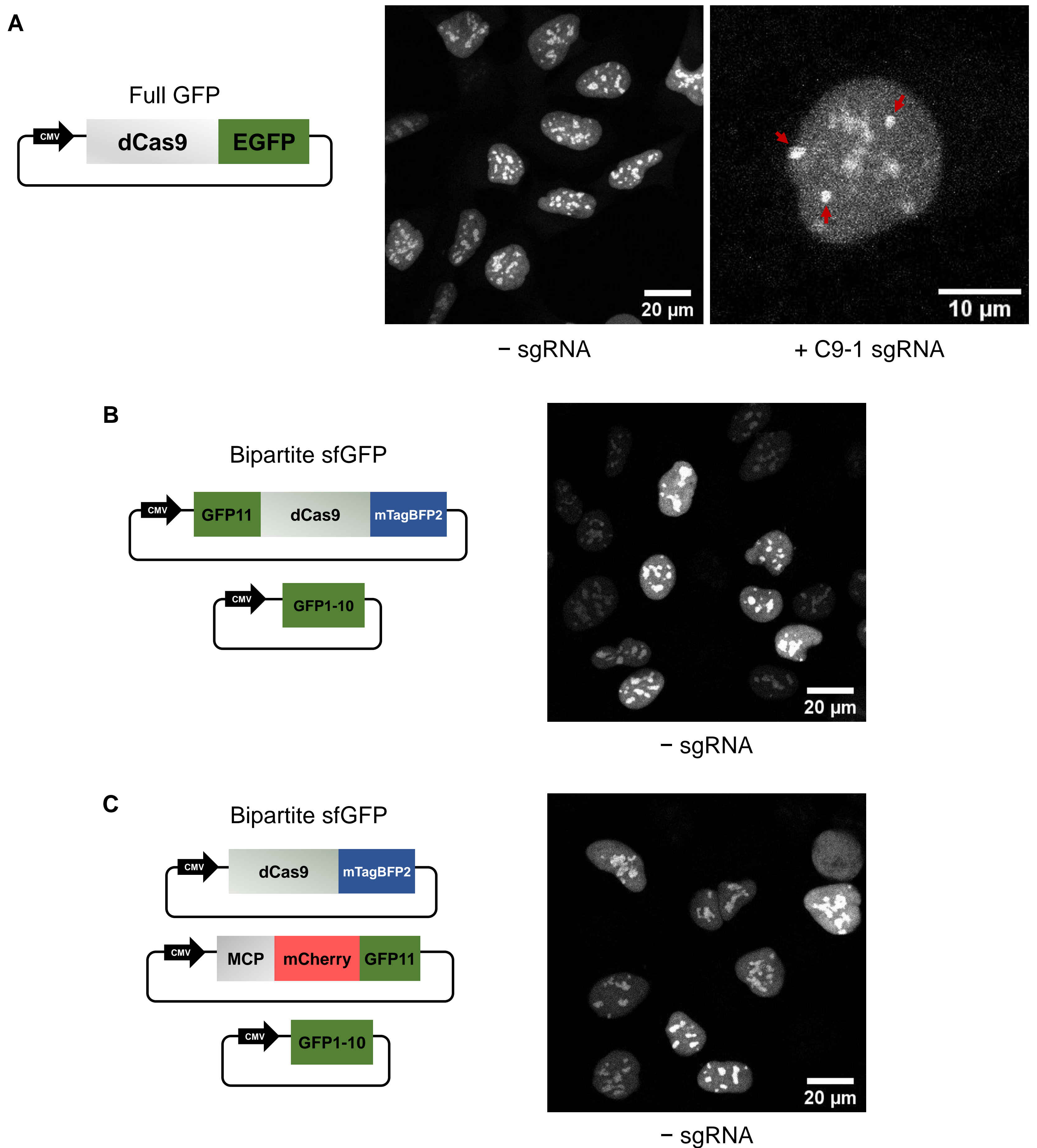
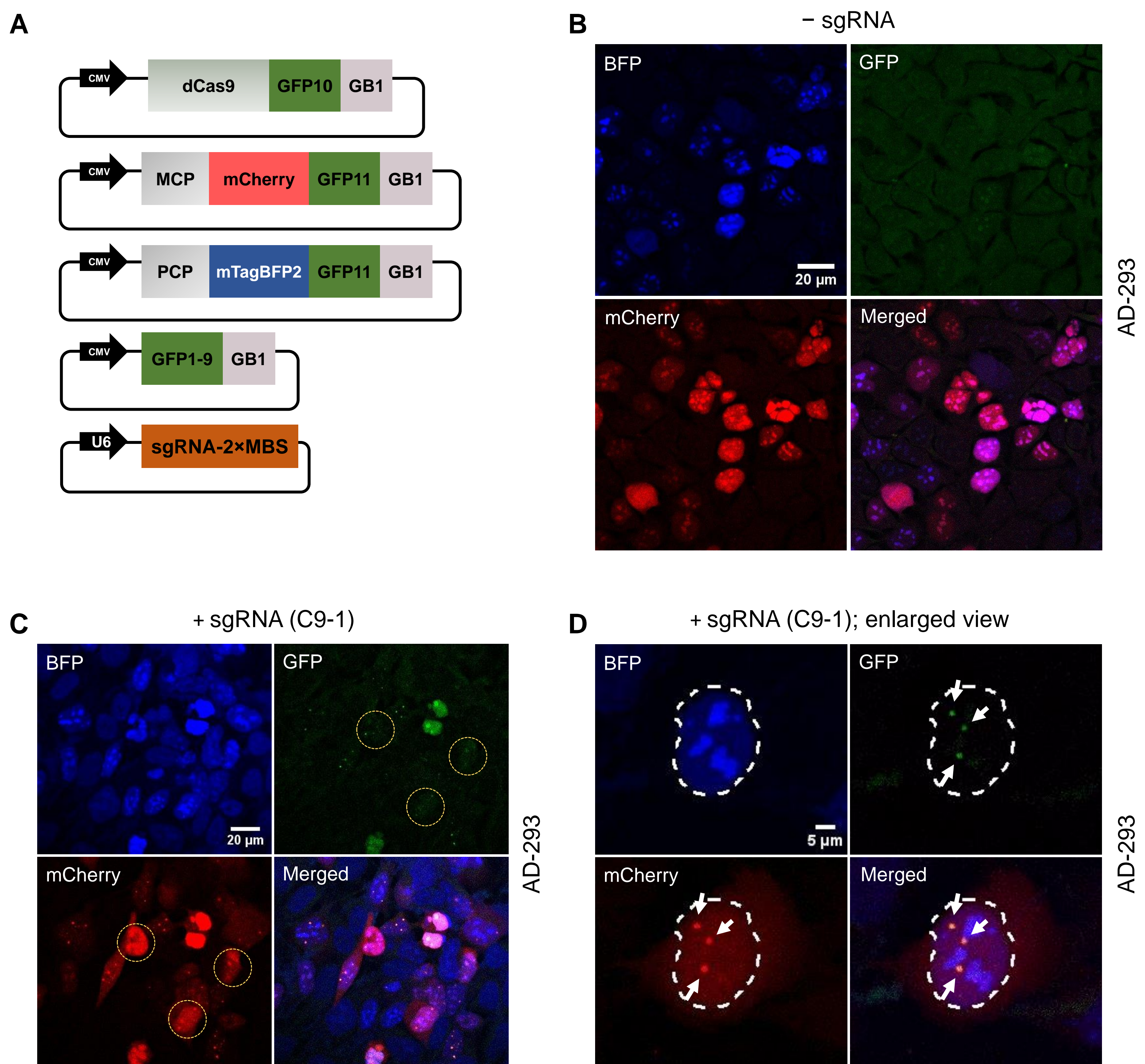


Supplemental Figure 1.



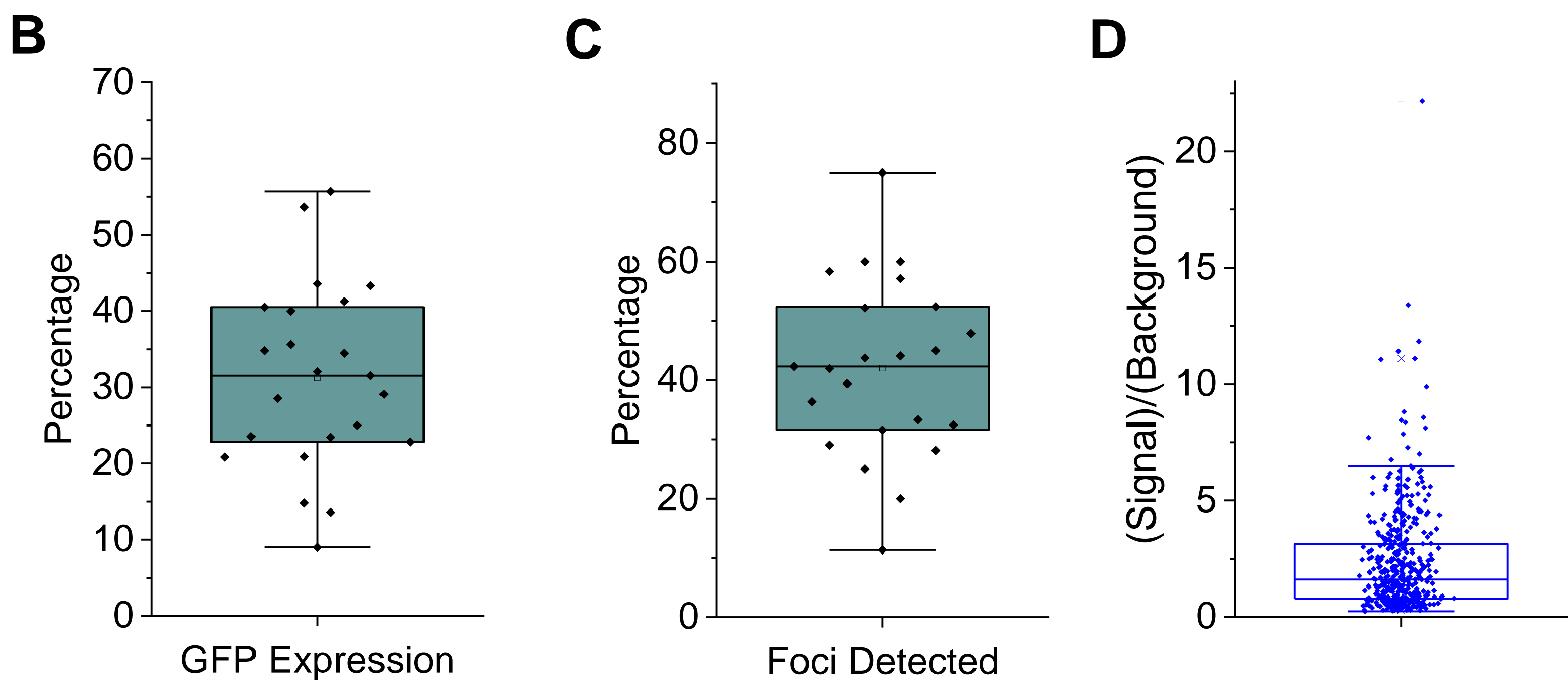
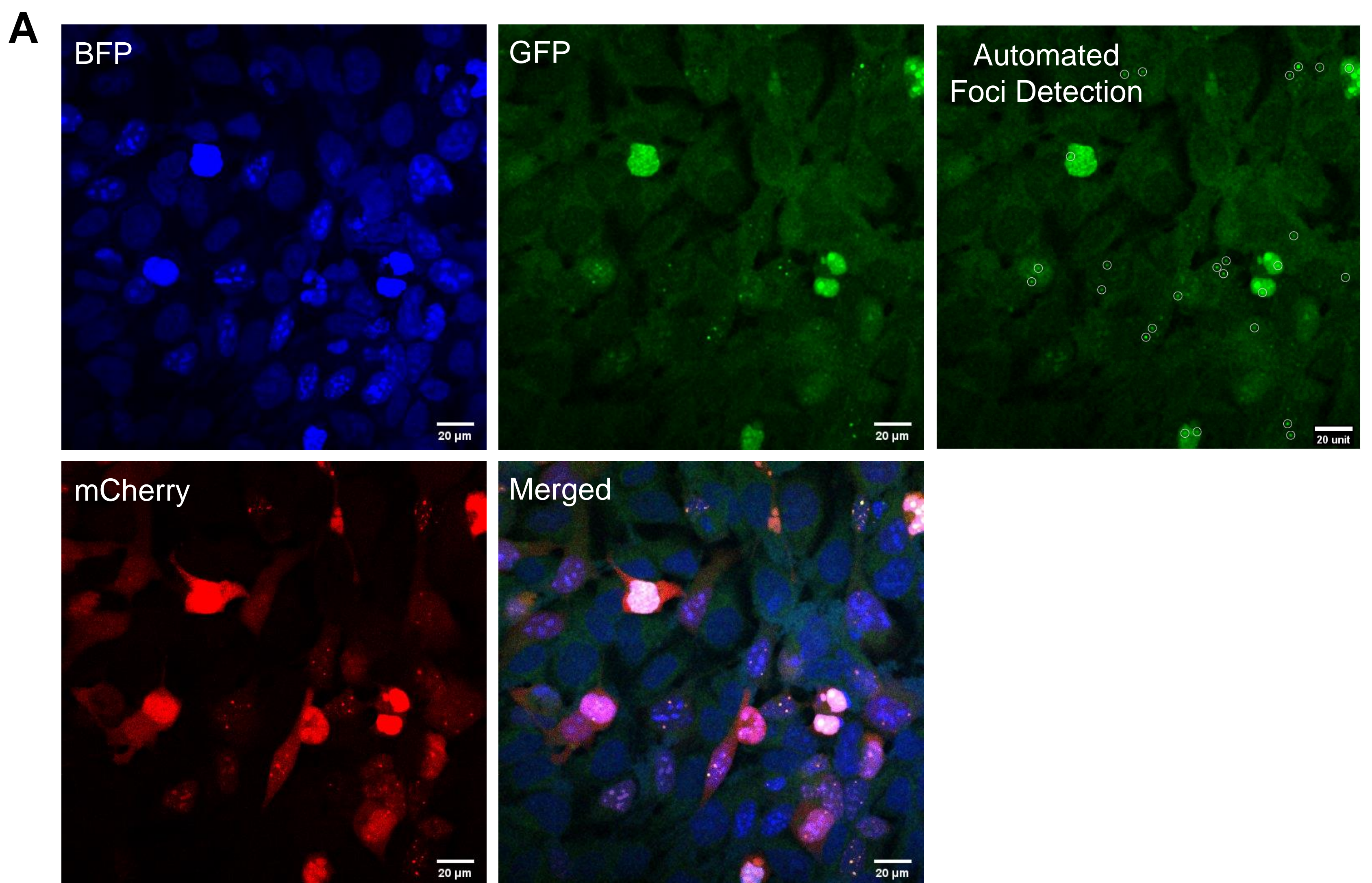
Supplemental Figure 1. Bipartite sfGFP designs exhibits heavy background signals. (A) The original design of dCas9 fused with EGFP (*left*). A representative image (GFP channel) in the absence of sgRNA showing background signals and non-specific foci in AD-293 cells (*right*). With sgRNA targeting C9-1 loci, potential target foci were observed (red arrows) but with considerable background signals. **(B)** A schematic design of dCas9 with bipartite sfGFP, where GFP11 was fused with dCas9 and GFP1-10 was expressed from a separate plasmid (*left*). A representative image (GFP channel) in the absence of sgRNA showing background signals similar to the full EGFP design (*right*). **(C)** Another schematic design of dCas9 with bipartite sfGFP, where GFP11 was fused with MCP to bind MS2 motifs in the tail of sgRNA and GFP1-10 was expressed from a separate plasmid (*left*). A representative image (GFP channel) in the absence of sgRNA showing similar background signals as the other designs (*right*).

Supplemental Figure 2.



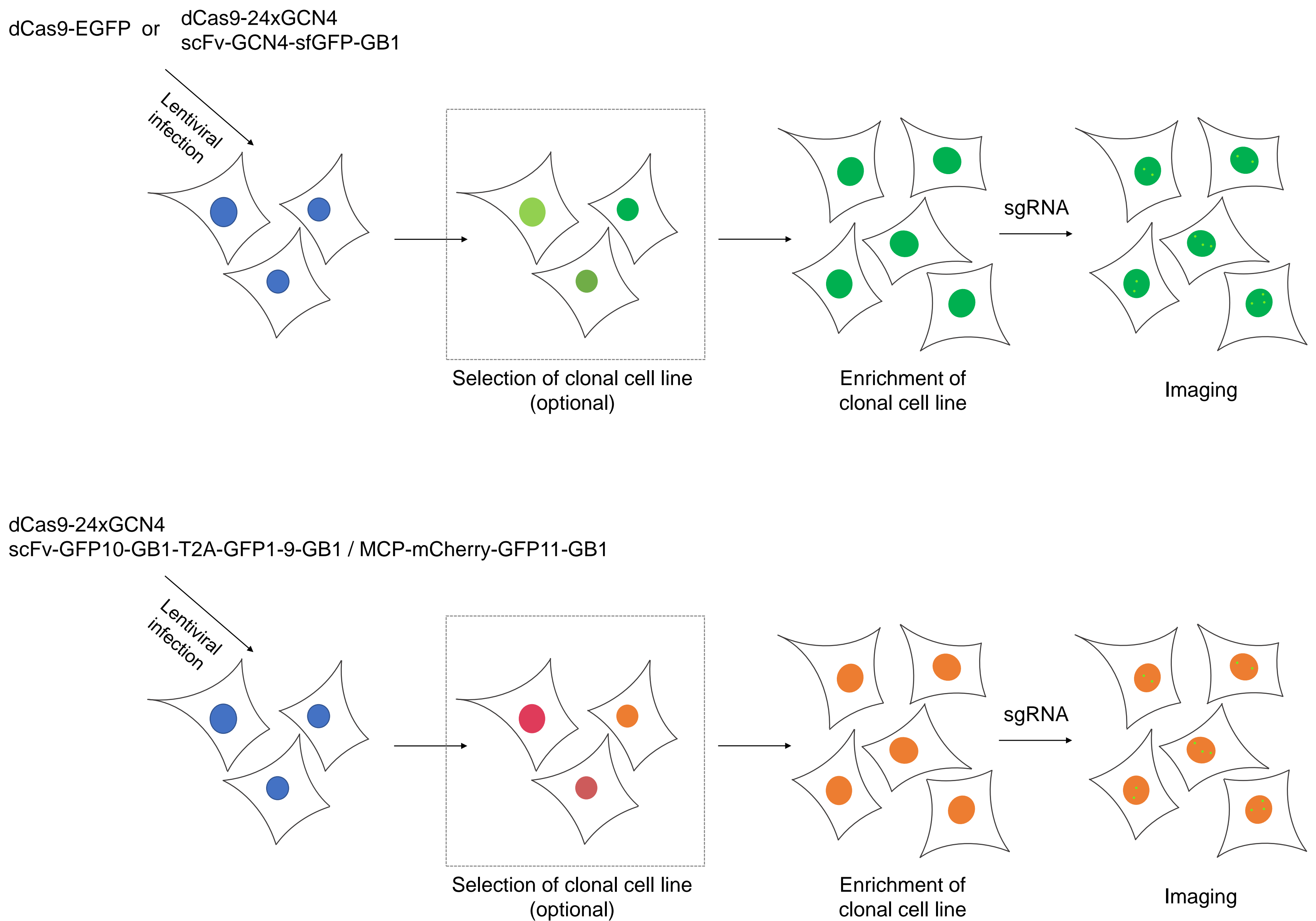
Supplemental Figure 2. Design and optimization of a tripartite sfGFP CRISPR system for suppressing background signals. **(A)** Schematic design of a CRISPR/dCas9 system with tripartite sfGFP. GFP10 and GFP11 were fused with dCas9 and MCP-mCherry, respectively. We used GFP11 fused with PCP to measure the signal from sgRNA-independent sfGFP assembly. GFP1-9 and sgRNA with 2×MBS targeting C9-1 loci were expressed in separate plasmids. **(B)** Representative images of AD-293 cells with all protein components but without sgRNA. BFP and mCherry channels revealed the high expression levels of proteins but GFP channel showed uniform and suppressed background level, due to the weak affinity between the sfGFP fragments. **(C)** Representative images acquired upon the transfection with C9-1 targeting sgRNA, showing target-specific foci in GFP and mCherry channels. BFP channel did not show target-specific foci, confirming that the foci in GFP and mCherry channels represent sgRNA-dependent assembly of the fluorophores. Even in the cells showing high background in mCherry channel, GFP channel revealed clear foci due to suppressed background (yellow circles). **(D)** Enlarged view of a cell nucleus showing three C9-1 foci in GFP and mCherry channels (white arrows).

Supplemental Figure 3.



Supplemental Figure 3. Estimation of transfection and loci detection efficiency. (A) Representative large field-of-view images from transient transfection of AD-293 cells with tripartite sfGFP CRISPR system and C9-1 targeting sgRNA. In the rightmost image, detected foci are marked with white circles. **(B)** Percentage of cells exhibiting GFP fluorescence calculated for 23 large field-of-view images. **(C)** Percentage of cells containing detected foci among those exhibiting GFP fluorescence in (B). **(D)** Scatter plot of S/B calculated for the detected foci.

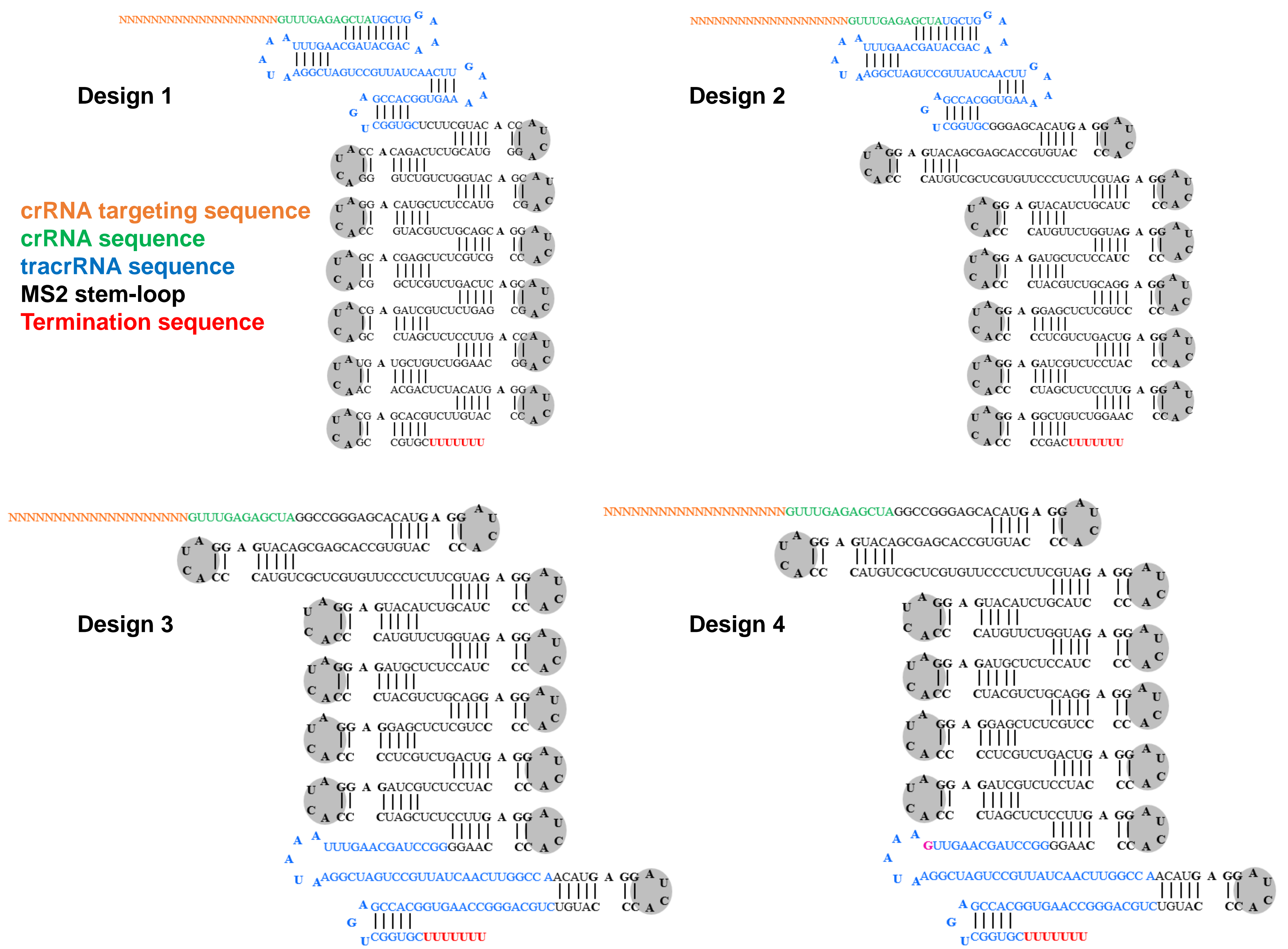
Supplemental Figure 4.



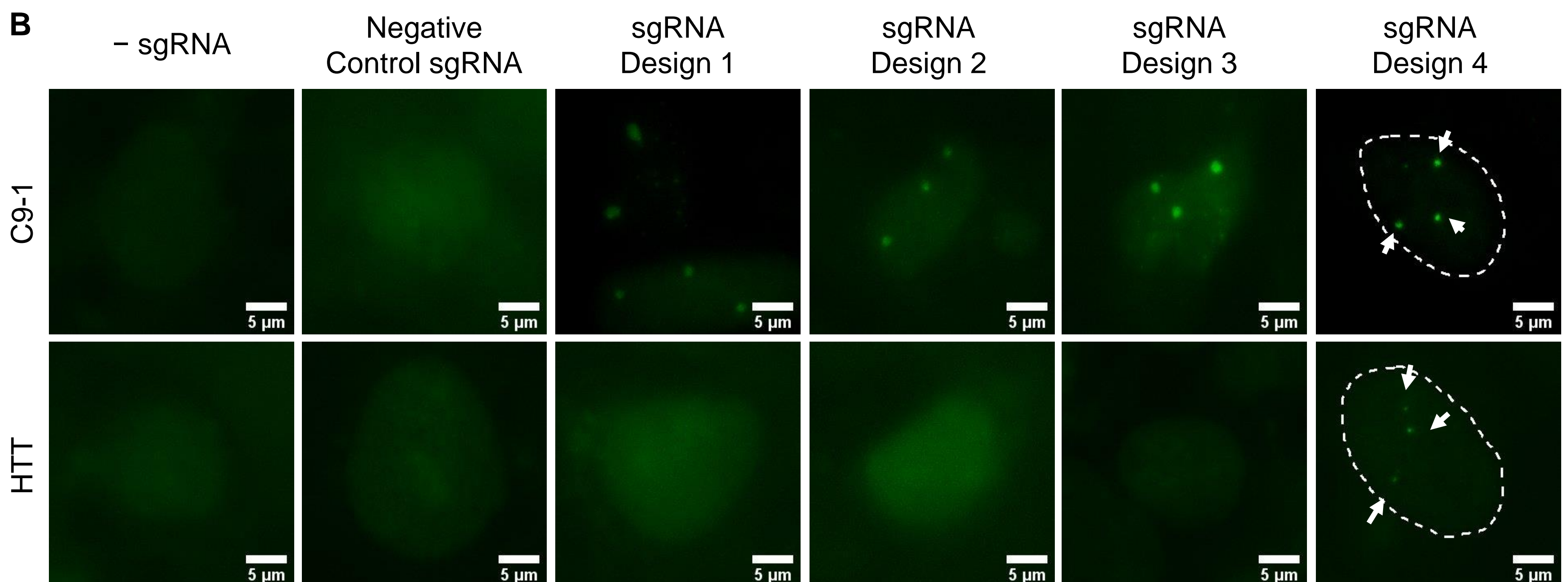
Supplemental Figure 4. Schematic process of selecting clonal cell lines used to make homogeneous stable cell lines with dCas9-EGFP, SunTag sfGFP, or SunTag split-sfGFP system. AD-293 cells were transfected with virus containing (1) dCas9-EGFP, (2) dCas9-24xGCN4 and ScFv-GCN4-sfGFP, or (3) dCas9-24xGCN4 and tripartite sfGFP components (scFv-GFP10, GFP1-9, and MCP-mCherry-GFP11). The tripartite sfGFP components could be expressed using a set of plasmids or using an all-in-one plasmid containing multiple components separated by self-cleaving peptide, T2A. After growing single colonies in 96 well-plates, single clones showing optimal expression levels of proteins were selected. Selected stable cell lines were later transfected transiently with sgRNA plasmids using Lipofectamine for visualizing target-specific foci.

Supplemental Figure 5.

A

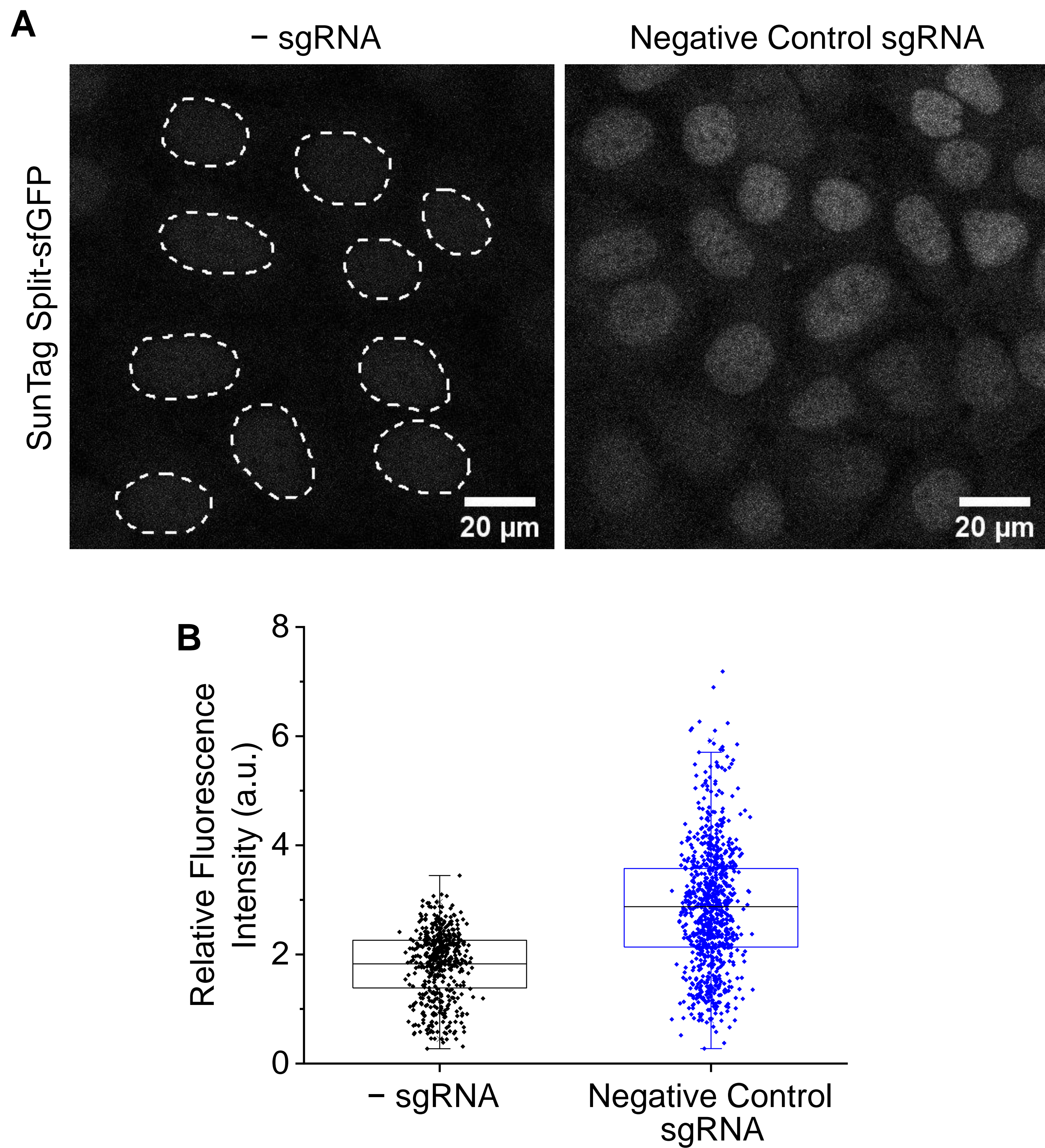


B



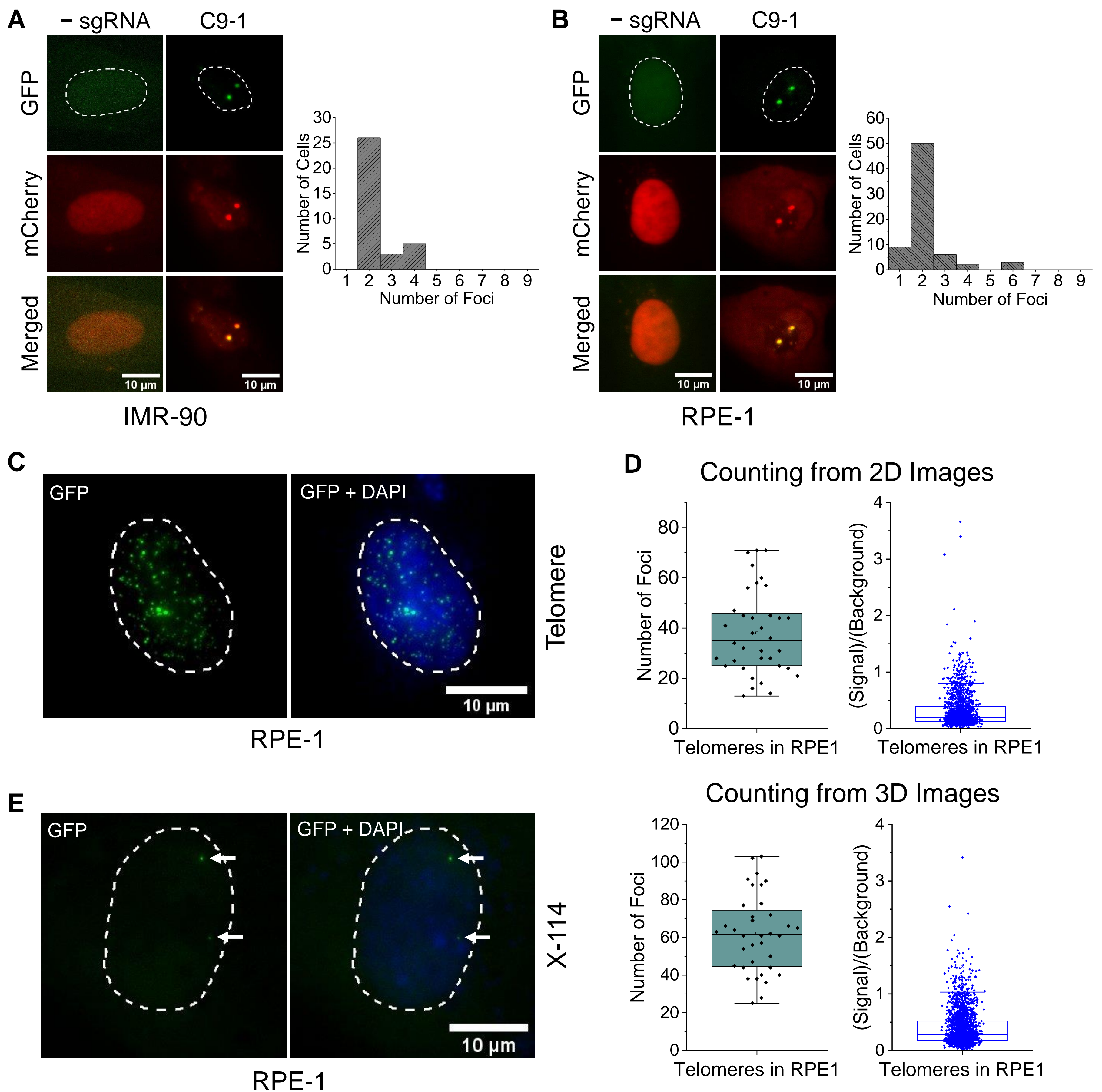
Supplemental Figure 5. Design and optimization of sgRNAs with 12×MBS. (A) Secondary structures of four different designs of sgRNA-12×MBS. Twelve MCP binding sites (MBS) were designed to avoid misfolding by using non-repeating stem sequences separated by linkers. The first three designs were made by making different arrangements of tracrRNA and linkers. The fourth design was further modified from the third by replacing an U with G (*magenta*), to avoid possible premature termination of transcription. **(B)** Representative images from labeling C9-1 and HTT loci using different designs of sgRNAs-12×MBS. Stable SunTag split-sfGFP AD-293 cell lines were transiently transfected with sgRNA plasmids. No clear foci were detected in the absence of sgRNA or with sgRNA targeting a random scrambled sequence. C9-1 loci were detected with all four sgRNA designs but HTT loci containing a small repeat region was successfully detected only with the fourth design.

Supplemental Figure 6.



Supplemental Figure 6. Dependence of fluorescence background level on the expression of sgRNA. (A) Representative large field-of-view images of GFP channel for the stable cell line without sgRNA (left) and with negative control sgRNA (right). The negative control sgRNA has a targeting sequence TTCCGCGTTACATAACTTA which does not have matching targets in the genome (Addgene plasmid #50927). The addition of sgRNA resulted in 1.6-fold increased background level, but not detectable foci. **(B)** Scatter plot of average fluorescence background level of individual nuclei from each condition (n = 506 nuclei for sgRNA (-); n = 864 nuclei for negative control sgRNA).

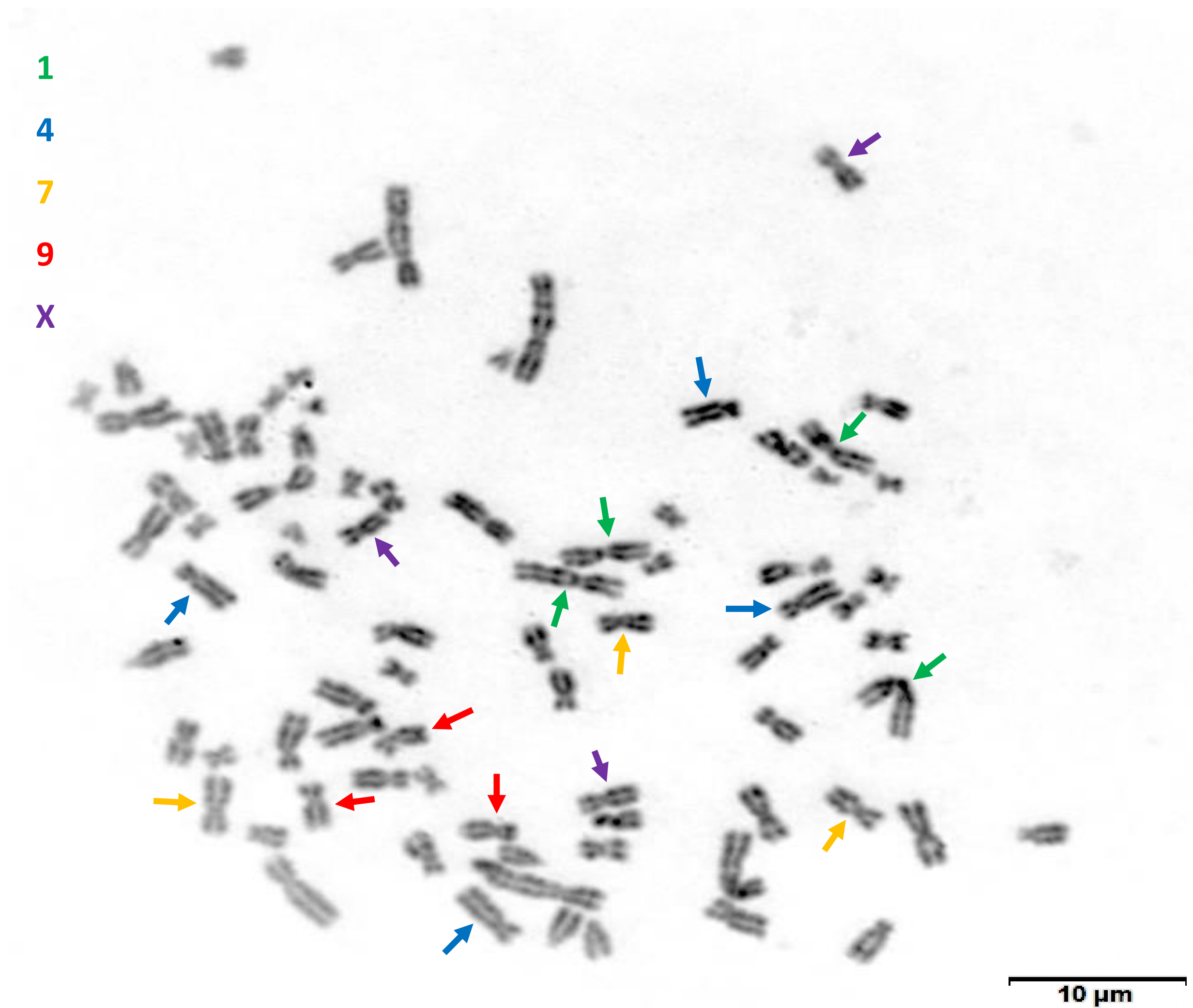
Supplemental Figure 7.



Supplemental Figure 7. Genomic loci imaging in different human cell lines using SunTag split-sfGFP. **(A)** Representative images of IMR-90 cells transfected with SunTag split-sfGFP CRISPR system and sgRNA-12xMBS targeting C9-1 loci, revealing two clear foci. Histogram shows the number of detected foci in IMR-90 cells ($n = 36$ cells). **(B)** Representative images of RPE-1 cells transfected with SunTag split-sfGFP CRISPR system and sgRNA-12xMBS targeting C9-1 loci, showing two clear foci. Histogram shows the number of detected foci in RPE-1 cells ($n = 70$ cells). **(C)** Representative images of telomeres in RPE-1 cells acquired using the same CRISPR system. **(D)** Results of counting telomeres in 2D images maximum-intensity-projected from z-stacked images and directly in 3D z-stacked images, shown along with respective S/B statistics ($n = 45$ cells). **(E)** Representative images of X-114 loci (*white arrows*) in RPE-1 cells acquired using the same CRISPR system.

Supplemental Figure 8.

A AD-293 SunTag split-GFP homogeneous stable cell line (Picture No. 1)



B

AD-293 wild-type cell line

Picture No.	Chr 1	Chr 4	Chr 7	Chr 9	Chr X
1	4	4	2	2	3
2	4	4	4	3	3
3	4	4	3	3	3
4	4	3	3	3	3
5	4	4	3	3	3
6	4	4	3	3	3
7	4	4	3	3	3
8	4	4	3	3	3
9	3	4	2	2	2
10	4	4	3	3	3
Average	3.9	3.9	2.9	2.8	2.9

AD-293 SunTag split-GFP homogeneous stable cell line

Picture No.	Chr 1	Chr 4	Chr 7	Chr 9	Chr X
1	4	4	3	3	3
2	4	4	3	3	3
3	4	4	3	3	4
4	4	4	2	4	3
5	4	4	2	2	3
6	4	4	3	3	3
7	4	4	3	2	3
8	4	4	3	3	3
9	4	4	3	3	3
10	3	4	3	3	3
Average	3.9	4.0	2.8	2.9	3.1

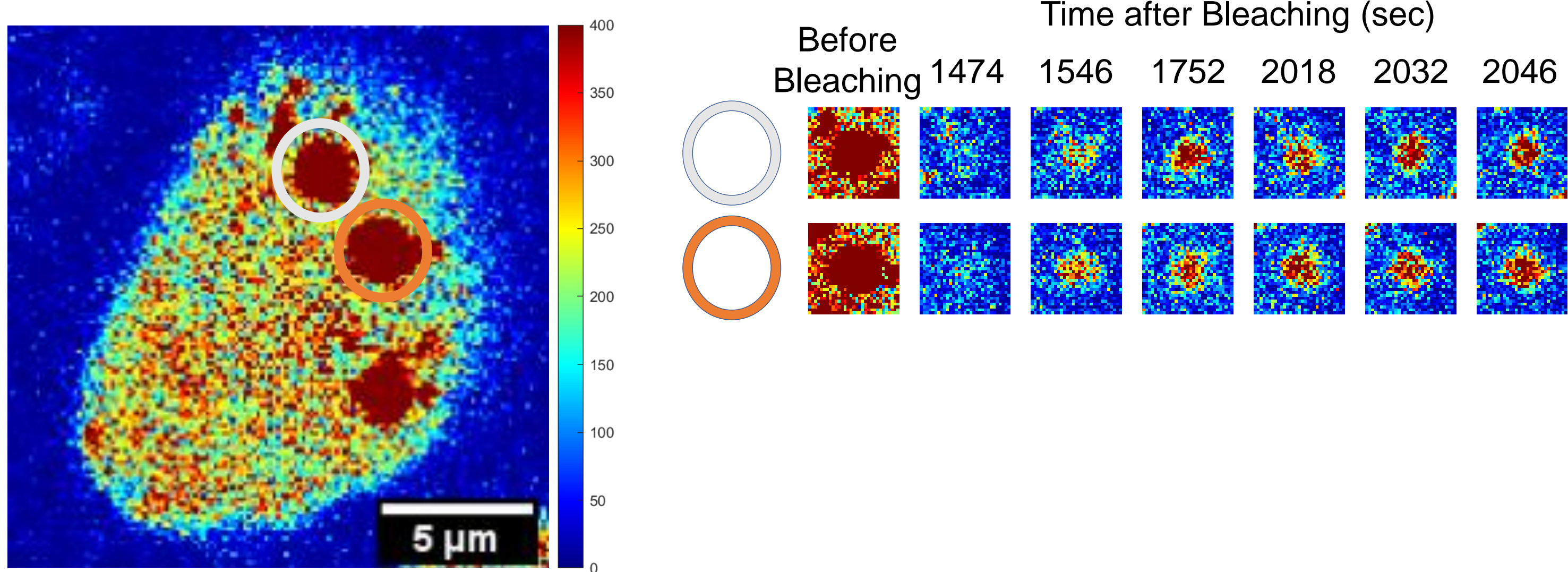
RPE-1 wild-type cell line

Picture No.	Chr 1	Chr 4	Chr 7	Chr 9	Chr X
1	2	2	2	2	2
2	2	2	2	2	2
3	2	2	2	2	2
4	2	2	2	2	2
5	2	2	2	2	2
6	2	2	2	2	2
7	2	2	2	2	2
8	2	2	2	2	2
9	2	2	2	2	2
10	2	2	2	2	2
Average	2.0	2.0	2.0	2.0	2.0

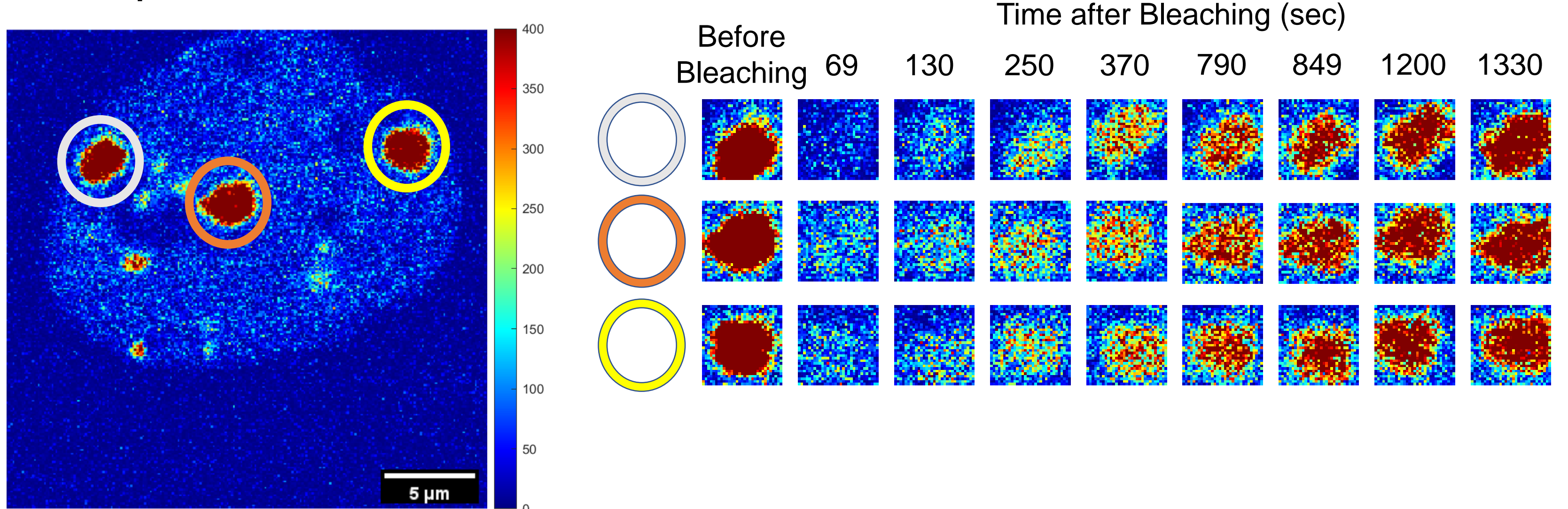
Supplemental Figure 8. Karyotyping analysis of chromosome copy numbers. (A) A representative karyotyping image of M phase chromosomes in an AD-293 cell containing SunTag split-sfGFP CRISPR system. Arrows indicate the identified Chromosomes 1, 4, 7, 9, and X. **(B)** Tables showing the number of identified chromosomes from the wild-type AD-293 cell line, the AD-293 homogeneous stable cell line with SunTag split-sfGFP CRISPR system, and the wild-type RPE-1 cell line. In both AD-293 cell lines, Chromosomes 1 and 4 were present in close to four copies while Chromosomes 7, 9, and X were present in close to three copies on average. In the RPE-1 cell line, all chromosomes were present in two copies.

Supplemental Figure 9.

Bipartite sfGFP

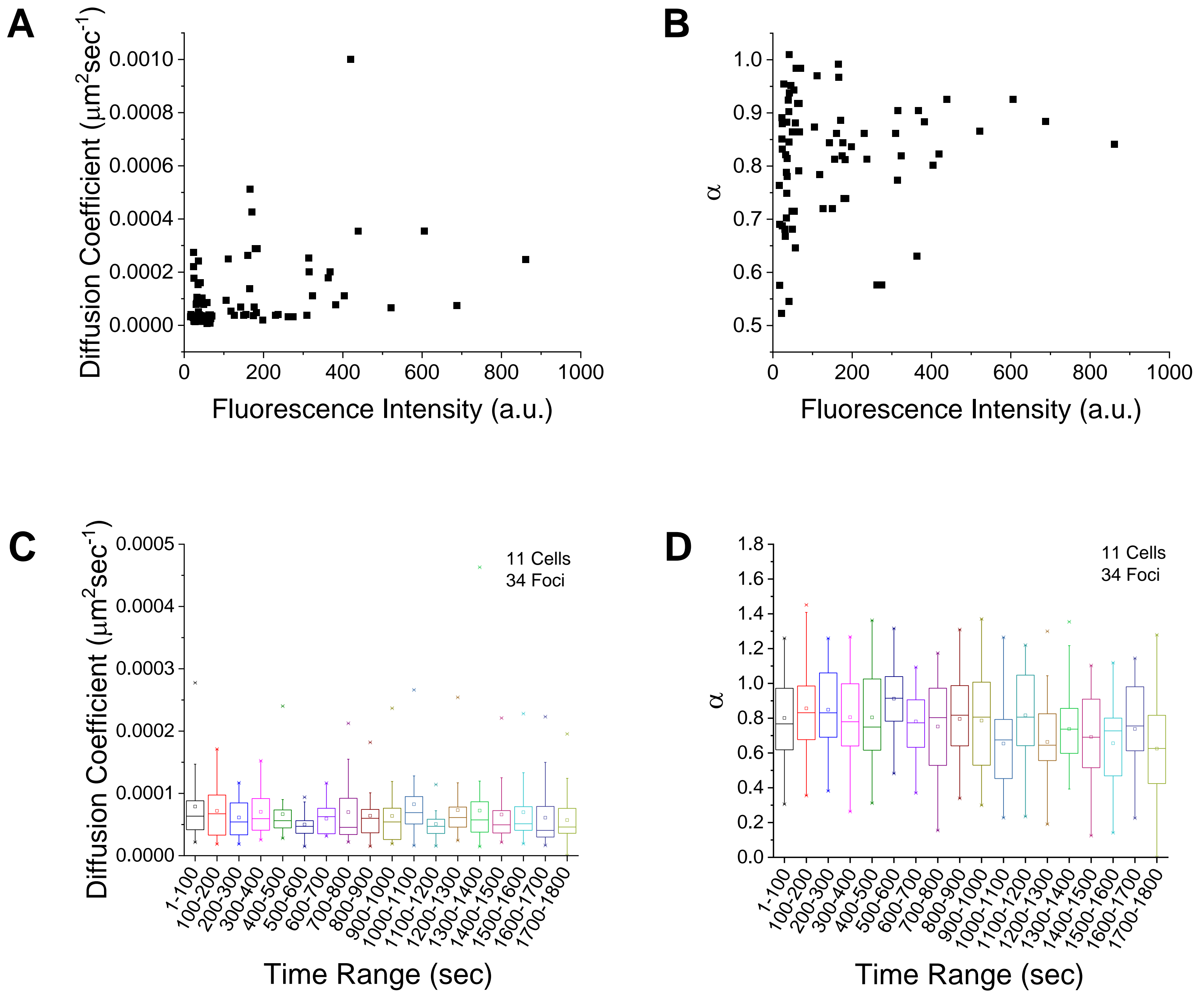


Tripartite sfGFP



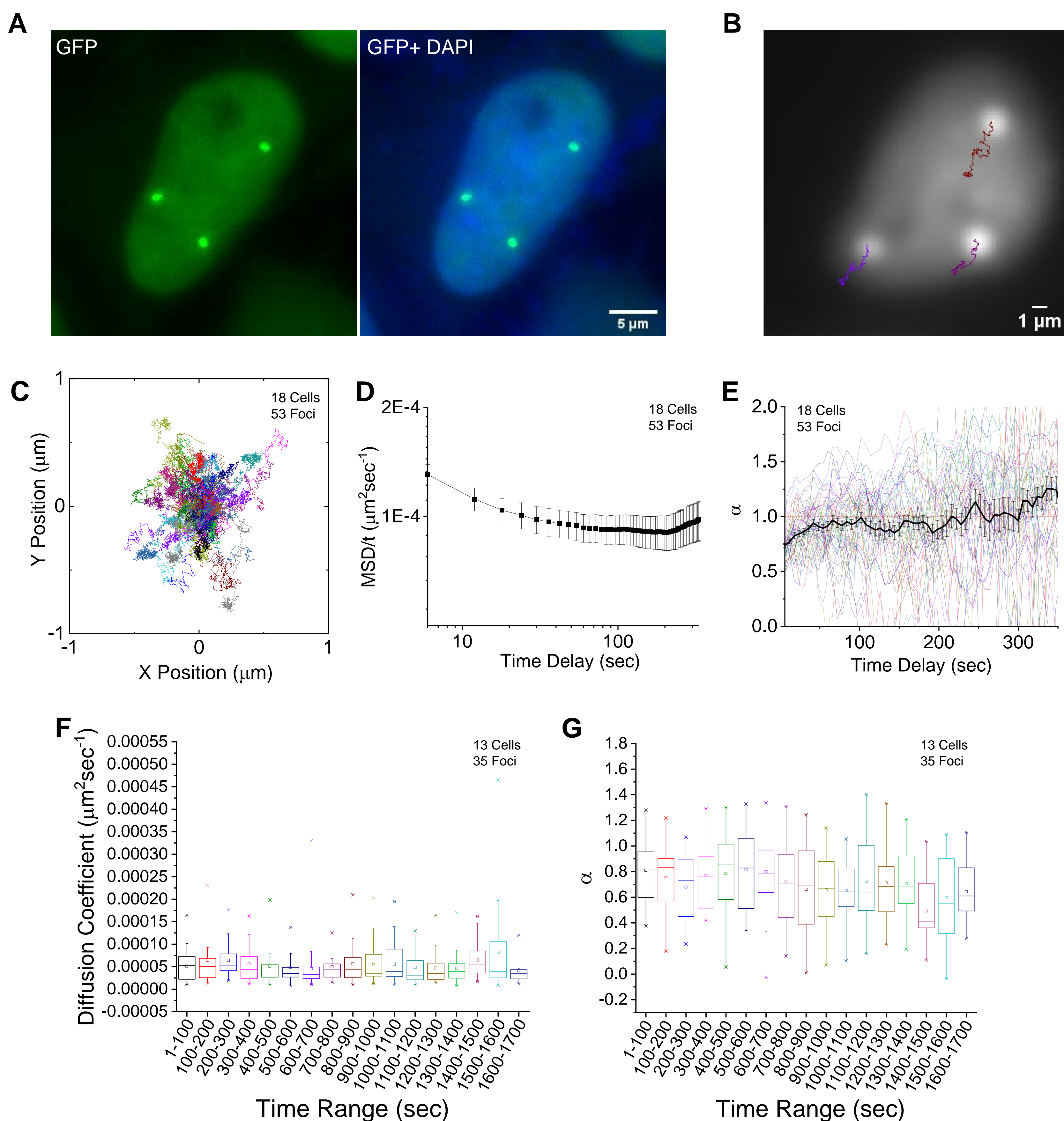
Supplemental Figure 9. Fluorescence recovery after photobleaching measurements on CRISPR-labeled genomic loci. Representative images of C9-1 foci with bipartite sfGFP and tripartite sfGFP are shown in the same absolute scale, along with time series of cropped images from each tracked focus. C9-1 foci with bipartite sfGFP could not be located in the initial period due to slow recovery.

Supplemental Figure 10.



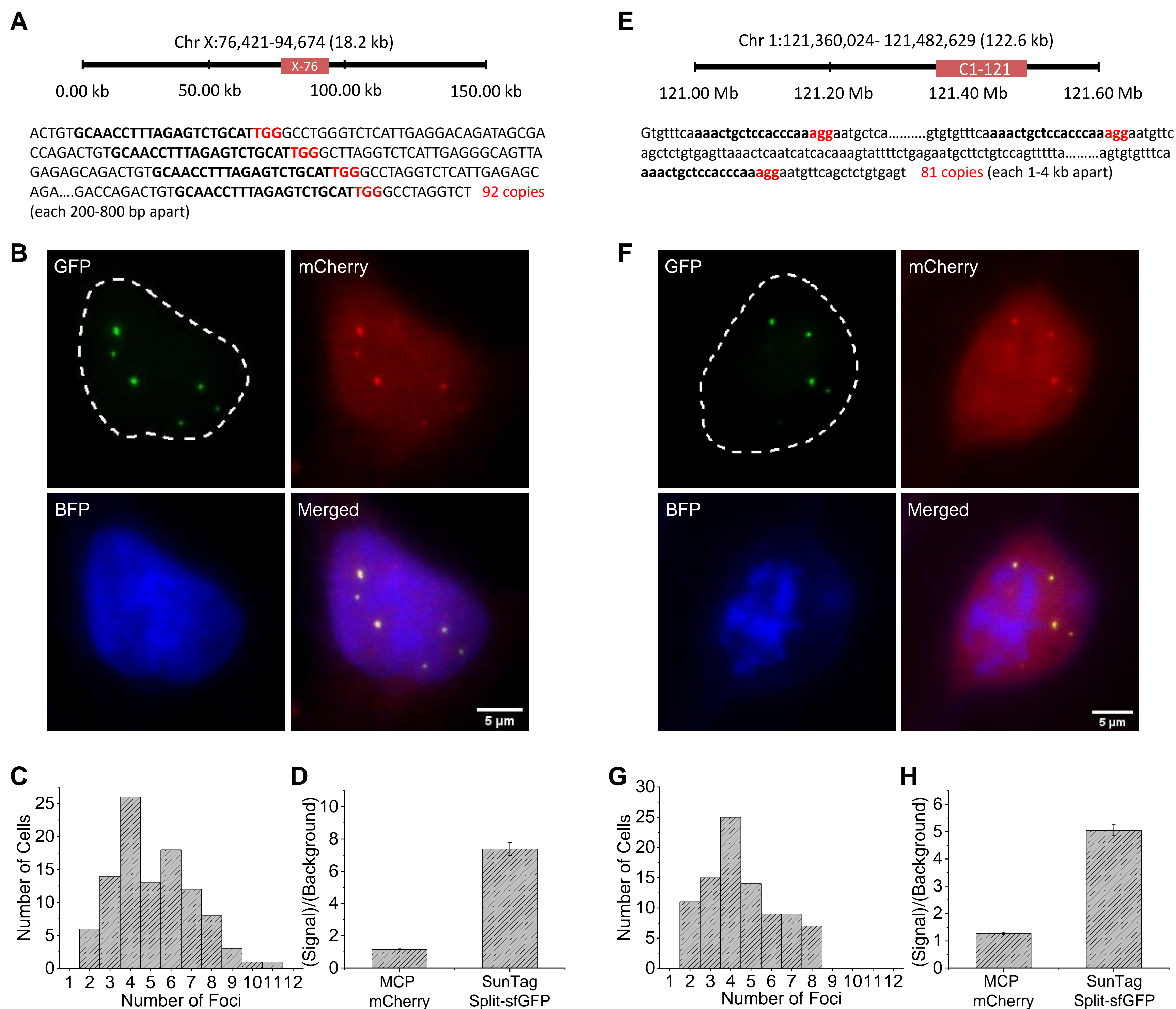
Supplemental Figure 10. Verification of diffusion trajectory data for possible effects of photo-irradiation. **(A)** Diffusion coefficient of the detected foci averaged over 330 sec, plotted against their initial signal intensities. **(B)** Diffusion exponent α of the detected foci plotted against their initial signal intensities. **(C, D)** Distribution of diffusion coefficient and diffusion exponent α of the trajectories measured in each 100 sec interval, for the purpose of checking the effect of extended photo-irradiation on the chromosomal dynamics.

Supplemental Figure 11.



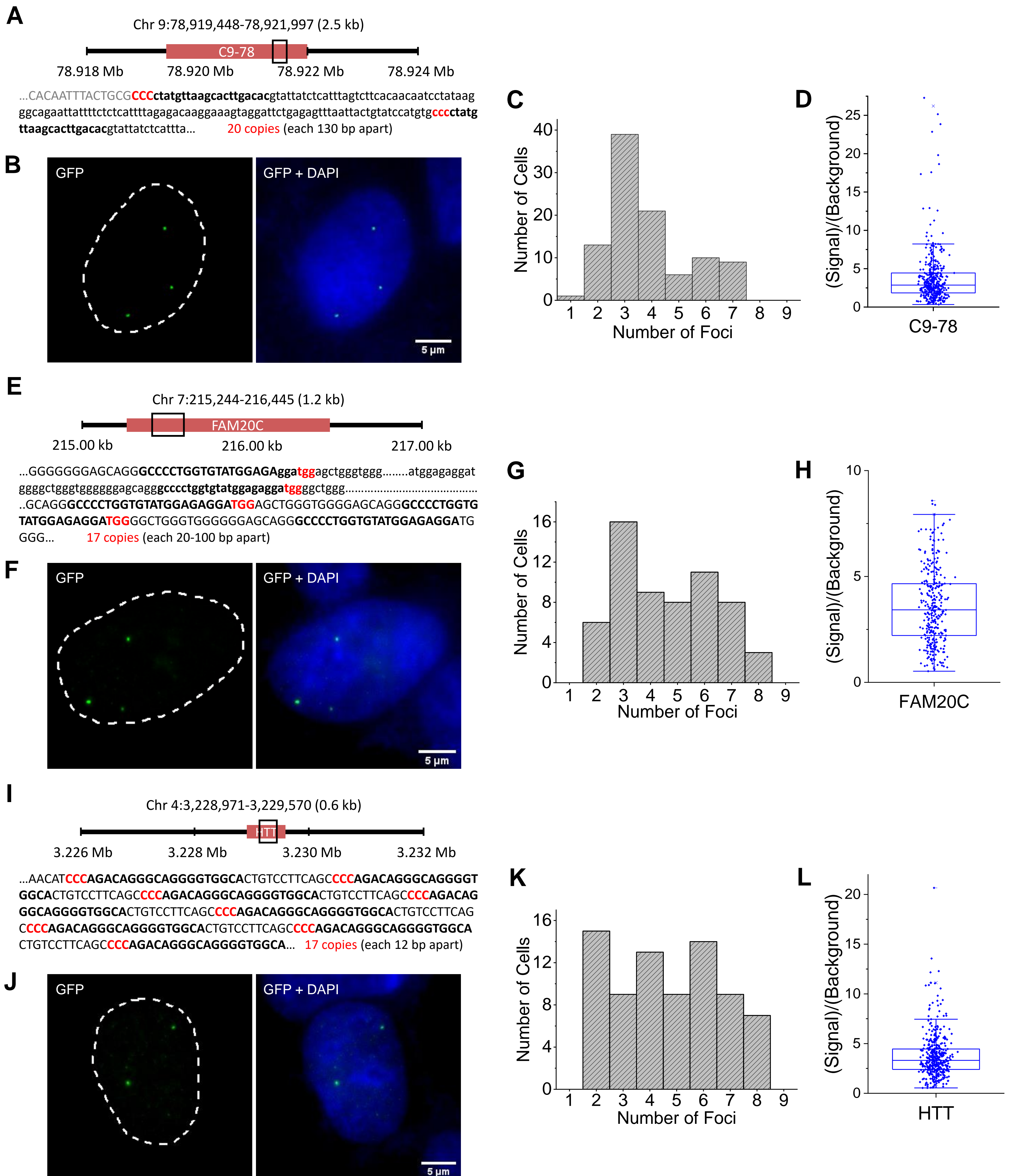
Supplemental Figure 11. Tracking C9-1 loci in AD-293 cells with SunTag sfGFP system. (A) Transfection of the colony-picked homogeneous stable SunTag sfGFP CRISPR AD-293 cell line with C9-1 sgRNA revealed three foci in most cells over substantial background signals. **(B)** Exemplary diffusion trajectory from a single cell shown with the first-frame image. **(C)** Collected trajectories of C9-1 foci shown over 330 sec (n = 53 loci). **(D)** MSD divided by time plotted over varying time delays for the trajectories in (C). Error bars represent s.e.m. between the observed foci. **(E)** Diffusion exponent α from MSD curves of the trajectories in (C) calculated for varying time delays. Trajectories traced for longer than 450 sec were taken for this analysis. Average and s.e.m. are shown in a black curve.

Supplemental Figure 12.



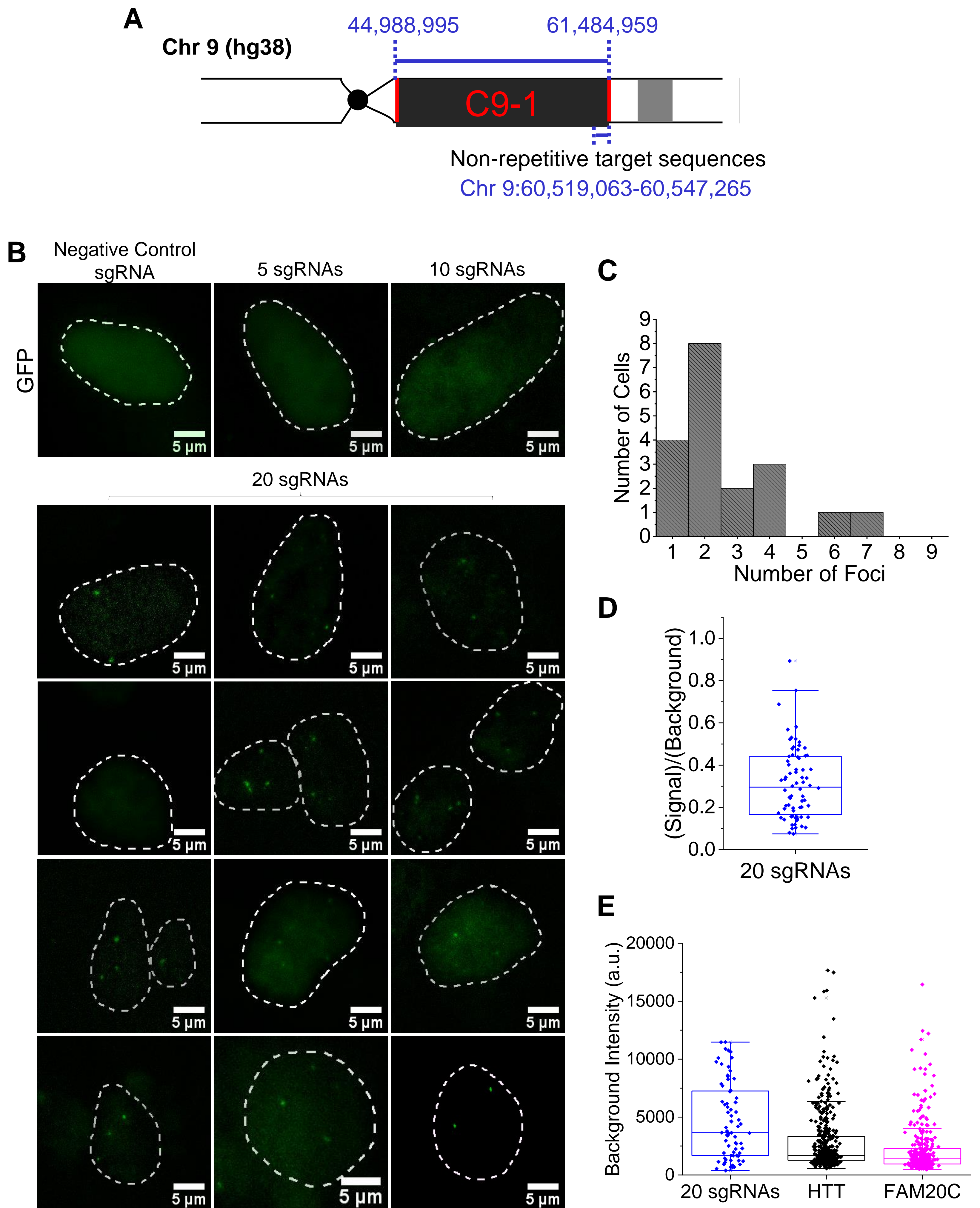
Supplemental Figure 12. Visualizing genomic loci of intermediate size in human Chromosome X and Chromosome 1. (A) Schematic diagram of X-76 locus in human Chromosome X containing 92 repeats of CRISPR target sequence (*bold*) with PAM sequence (*red*). Sequence is shown for the black-boxed area. (B) Representative images of X-76 loci in AD-293 cells acquired using the homogeneous stable cell line with SunTag split-sfGFP CRISPR system. (C) Histogram of the number of detected X-76 foci in AD-293 cells. (D) Comparison of S/B of the X-76 foci imaged with MCP-mCherry and SunTag split-sfGFP. (E) Schematic diagram of C1-121 locus in human Chromosome 1 containing 81 repeats of CRISPR target sequence (*bold*) with PAM sequence (*red*). Sequence is shown for the black-boxed area. (F) Representative images of C1-121 loci in AD-293 cells acquired using the homogeneous stable cell line with SunTag split-sfGFP CRISPR system. (G) Histogram of the number of detected C1-121 foci in AD-293 cells. (H) Comparison of S/B of the C1-121 foci imaged with MCP-mCherry and SunTag split-sfGFP.

Supplemental Figure 13.



Supplemental Figure 13. Visualizing small-repeat genomic regions with SunTag split-sfGFP CRISPR system. (A) Schematic diagram of C9-78 locus in human Chromosome 9 containing 20 repeats of CRISPR target sequence (*bold*) with PAM sequence (*red*). Sequence is shown for the black-boxed area. (B) Representative images of C9-78 loci in AD-293 cells acquired using the homogeneous stable cell line with SunTag split-sfGFP CRISPR system. (C) Histogram of the number of detected C9-78 foci in AD-293 cells. (D) Scatter plot of S/B for the detected foci. (E-H) Same measurements and analyses as (A-D) for FAM20C gene locus in human Chromosome 7 containing 17 repeats of CRISPR target. (I-L) Same measurements and analyses as (A-D) for HTT gene locus in human Chromosome 4 containing 17 repeats of CRISPR target.

Supplemental Figure 14.



Supplemental Figure 14. Visualizing a non-repeat genomic region with SunTag split-sfGFP CRISPR system. (A) Schematic showing the targeted region with 20 sgRNAs (**Supplemental Table 2**). **(B)** Representative images of the non-repeat region labeled with 5, 10, and 20 sgRNAs, along with an image with negative control sgRNA. **(C)** Histogram of the number of foci per cell detected with 20 sgRNAs. **(D)** Scatter plot of S/B for the detected foci. **(E)** Scatter plot of individual average background intensity of detected foci, compared between the non-repeat region with 20 sgRNAs, HTT, and FAM20C region.

Supplemental Table 1.

Target	Guide Sequence_PAM (NGG)	# of Repeats	Location (GRCh37/hg19)	Location (GRCh38/hg38)
Telomere	GTTAGGGTTAGGGTTAGGGTT_AGG	NA	-	-
C9-1	GTGGAATGGAATGGAATGGAA_TGG	NA	-	-
FAM20C	GCCCCTGGTGTATGGAGAGGA_TGG	17	Chr 7:215244-216445	Chr 7:215244-216445
HTT	CCA_GACAGGGCAGGGGTGGCACTG	17	Chr 4:3228971-3229570	Chr 4:3227241-3227839
C9-78	CCC_CTATGTTAAGCACTTGACAC	20	Chr 9:78919448-78921997	Chr 9:76304532-76307081
X-114	AAATGCCAGCGGAAAGTCCA_TGG	13	Chr X:114962601-114998453	Chr X:115846268-115882117
X-1	GCAACCTTTAGAGTCTGCAT_TGG	92	Chr X:76421-94674	Chr X:26299-44674
C1-121	AAACTGCTCCACCCAA_AGG	81	Chr 1:121360024- 121482629	Chr 1:121616360-121740831
Scrambled sgRNA (negative control)	GTTCCGCGTTACATAACTTA	None	None	None

Supplemental Table 1. sgRNA target sequences of the genomic regions imaged in this study, shown along with the number of repeats and the chromosomal location.

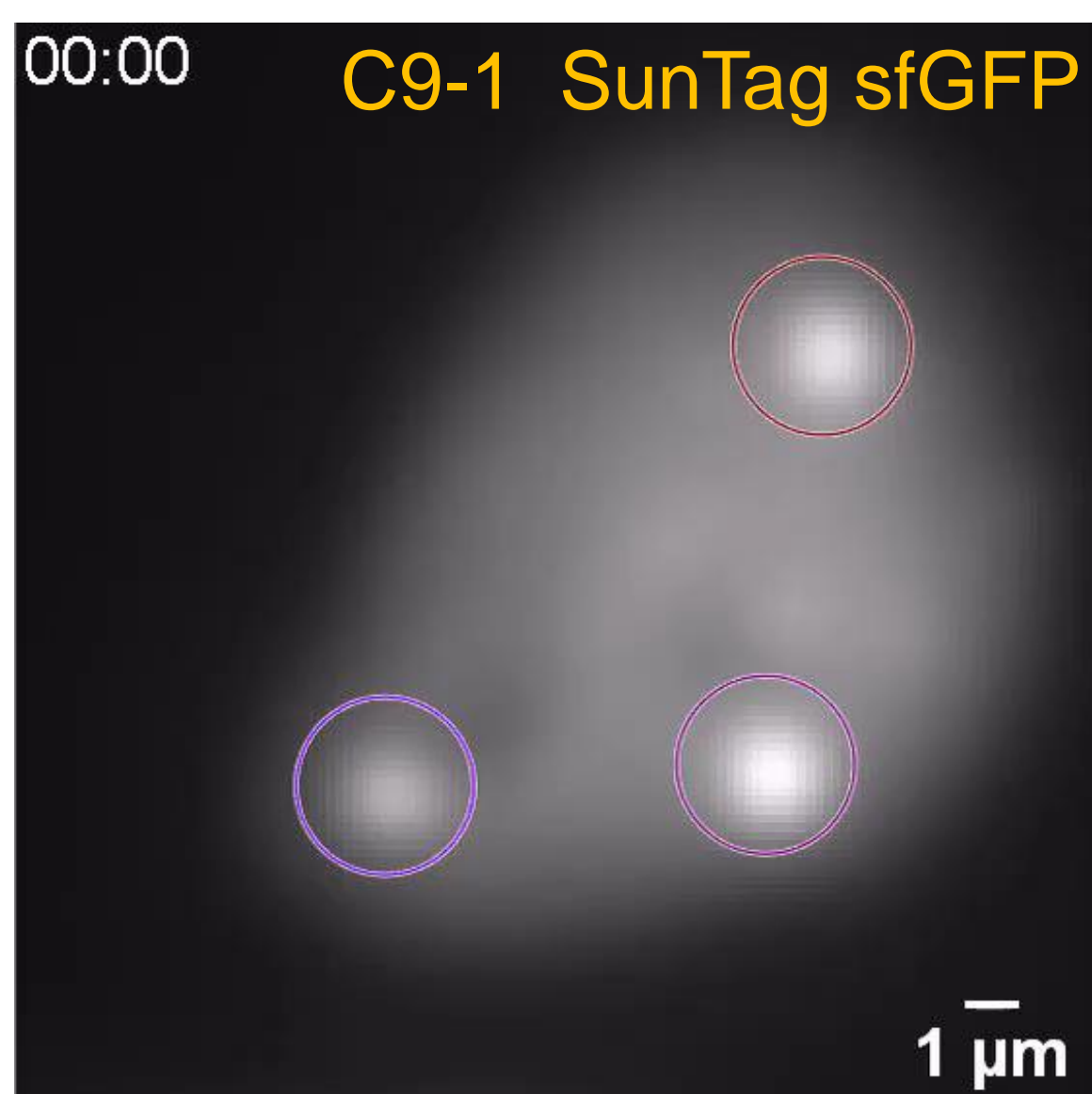
Supplemental Table 2.

Serial Number	Guide Sequence_PAM (NGG)	Location (hg38)
9q12-d #1	AGACAGTAGTACCAGTGTTT_TGG	Chr 9:60519063-60519085
9q12-d #2	AGACCACAGCAGGGTTGTTT_TGG	Chr 9:60519875-60519897
9q12-d #3	AGACTCAAGCATCAGTGTTT_TGG	Chr 9:60522988-60523010
9q12-d #4	TGAATGTTTGTTCCTTACAG_GGG	Chr 9:60523921-60523943
9q12-d #5	GTATTCAGGAATCCTATATT_AGG	Chr 9:60524341-60524363
9q12-d #6	CTTTGAGGCCTAACGTGGAA_AGG	Chr 9:60532108-60532130
9q12-d #7	TTTGACACCTATGGTCGAAA_AGG	Chr 9:60533130-60533152
9q12-d #8	TGGTCTATGTATGGTAGATA_AGG	Chr 9:60535518-60535537
9q12-d #9	GAGCGGTTTGAGGCCTATCC_TGG	Chr 9:60541359-60541378
9q12-d #10	GAACGCTTTGGGGCCTATCA_TGG	Chr 9:60543234-60543256
9q12-d #11	AGGCCATGTGGAGAGCTTTG_AGG	Chr 9:60543758-60543777
9q12-d #12	AGAGTGCAGGACCTGGCACT_TGG	Chr 9:60545789-60545811
9q12-d #13	AGCGCAGCCTGTCGGGCCCT_GGG	Chr 9:60545842-60545864
9q12-d #14	GTTCCCCTGGGATGGCCTCC_TGG	Chr 9:60546141-60546160
9q12-d #15	GCTCGGGCTCTGGCAGAGGC_TGG	Chr 9:60546168-60546187
9q12-d #16	GCAGAAATCGCCGCCTGCAC_TGG	Chr 9:60546500-60546522
9q12-d #17	CTGTTGCGCGGGGCCAGCTA_AGG	Chr 9:60546564-60546586
9q12-d #18	GCAGTGCTGAGTCTGTGCAA_AGG	Chr 9:60546641-60546660
9q12-d #19	TGGAGCAATTTGACGCCTA_CGG	Chr 9:60547313-60547332
9q12-d #20	GCACCGCCGCAGGCACCAGG_AGG	Chr 9:60547246-60547265

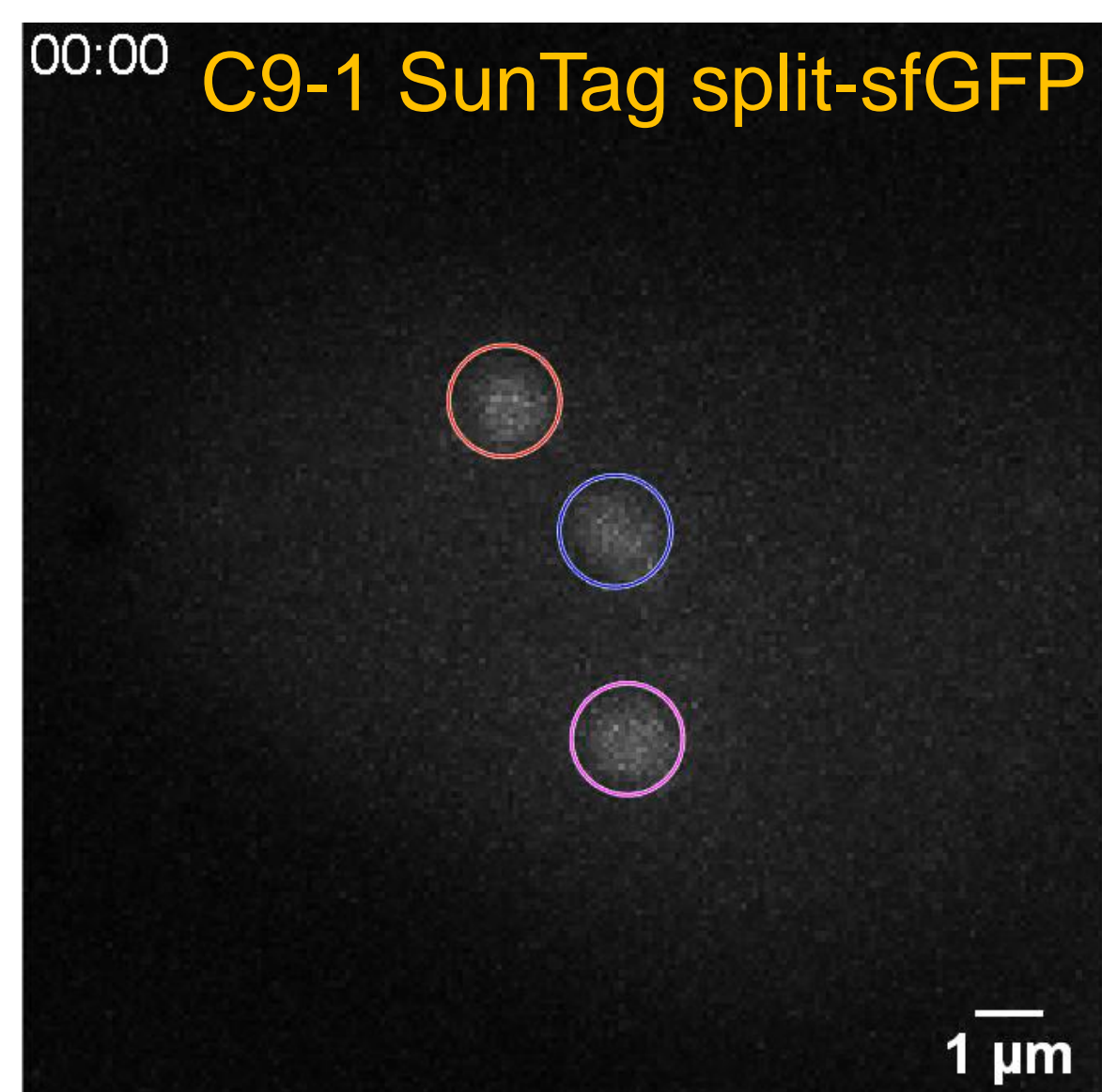
Supplemental Table 2. sgRNA sequences targeting non-repetitive genomic region downstream of 9q12 of the human genome (GRCh38/hg38).

List of Supplemental Movies.

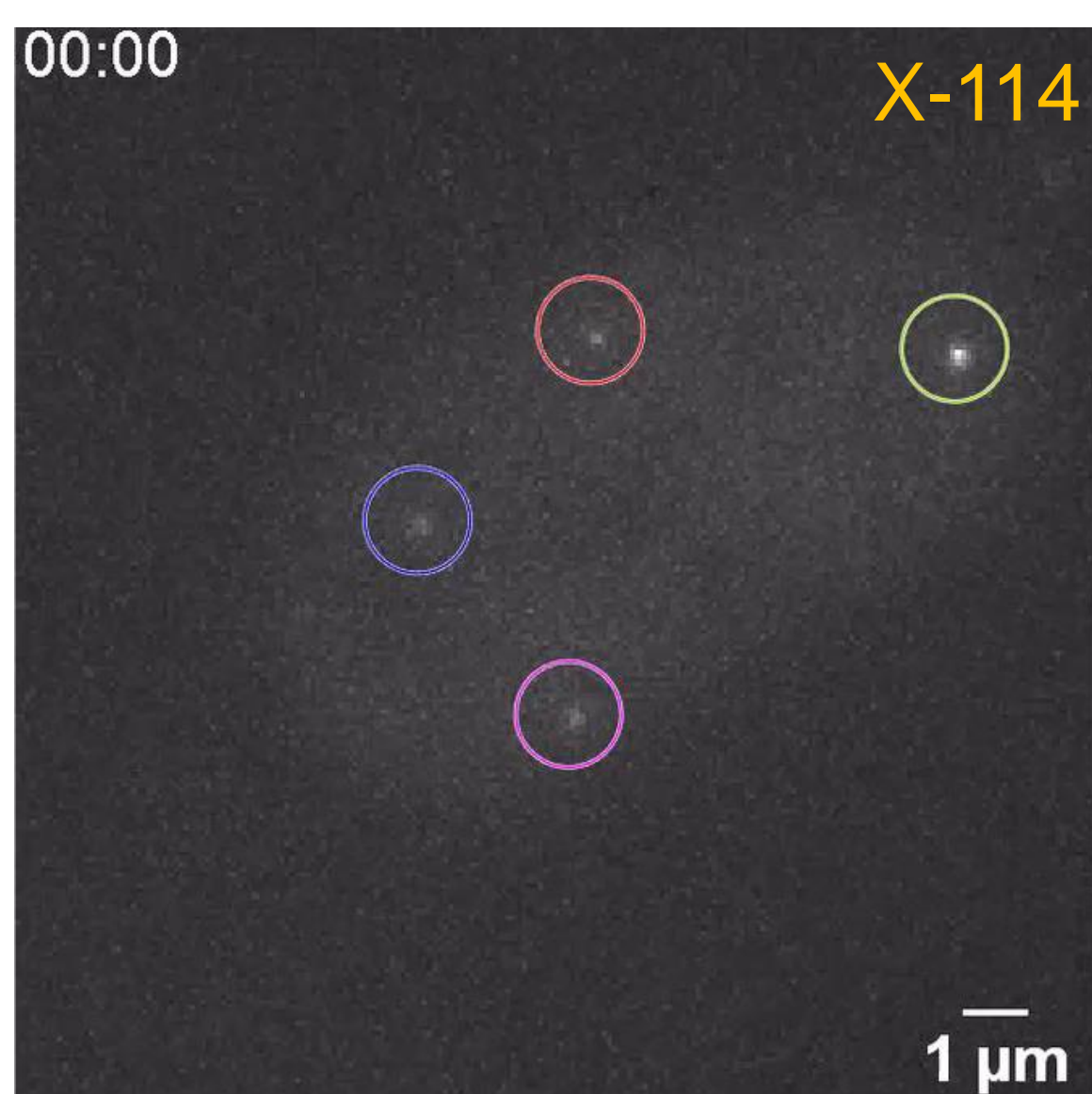
Supplemental Movie 1.



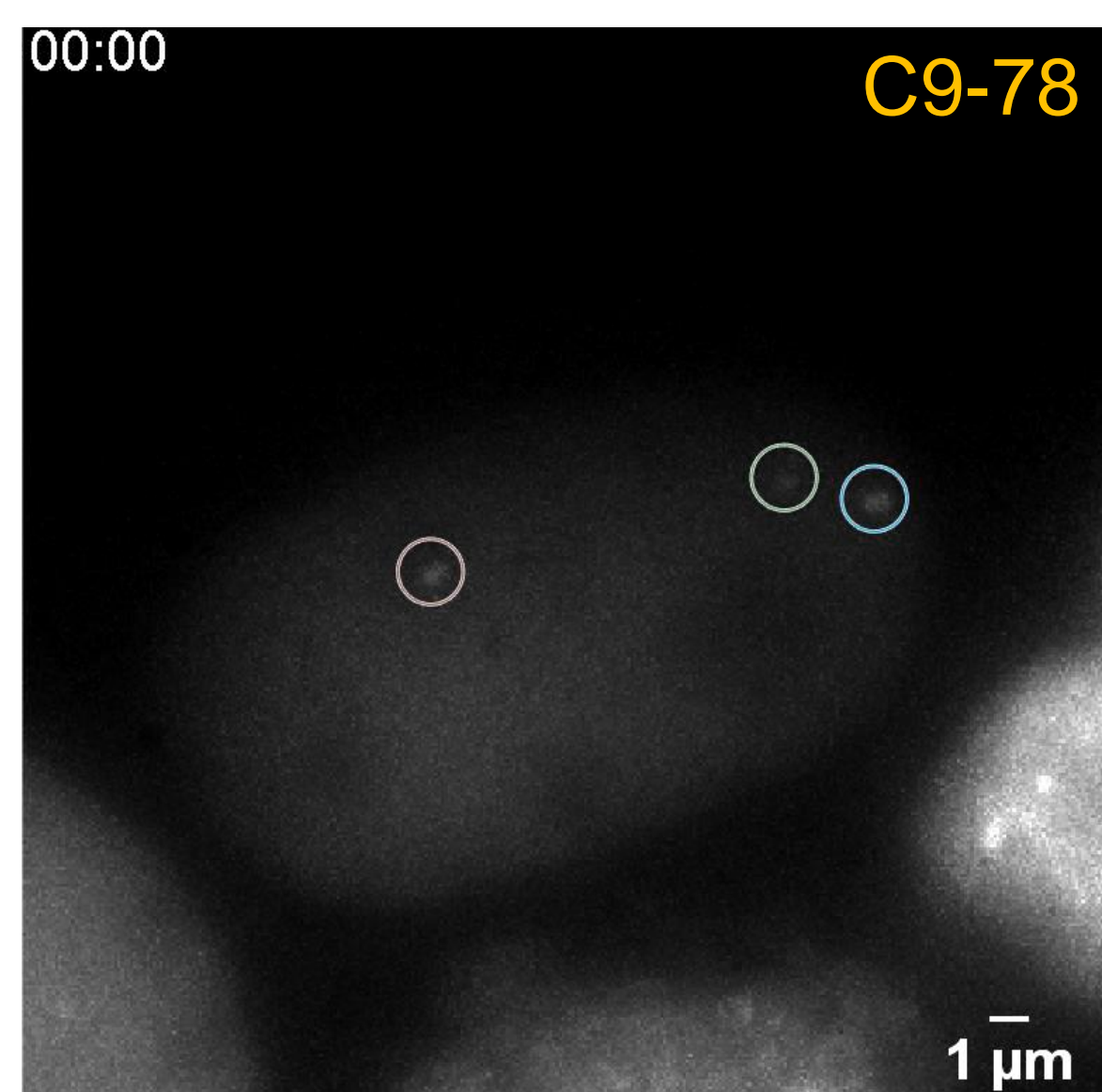
Supplemental Movie 2.



Supplemental Movie 3.



Supplemental Movie 4.



Supplemental Movie 1. A representative movie of C9-1 foci imaged with SunTag sfGFP and 12×MBS-sgRNAs in AD-293 cells. Detected foci are marked with circles and trajectories are shown along time. Time is displayed in minutes: seconds.

Supplemental Movie 2. A representative movie of C9-1 foci imaged with SunTag split-sfGFP and 12×MBS-sgRNAs in AD-293 cells. The movie was taken with the same imaging condition and displayed in the same scale of brightness as in Supplemental Movie 1.

Supplemental Movie 3. A representative movie of X-114 foci (DXZ4 gene) imaged with SunTag split-sfGFP and 12×MBS-sgRNAs in AD-293 cells.

Supplemental Movie 4. A representative movie of C9-78 foci imaged with SunTag split-sfGFP and 12×MBS-sgRNAs in AD-293 cells.